

Theoretical Study of the Energetics of Proton Pumping and Oxygen Reduction in Cytochrome Oxidase

Per E. M. Siegbahn,* Margareta R. A. Blomberg,* and Mattias L. Blomberg

Department of Physics, Stockholm Centre for Physics, Astronomy and Biotechnology (SCFAB), Stockholm University, S-106 91 Stockholm, Sweden

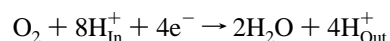
Received: May 28, 2003

Hybrid density functional theory using the B3LYP functional has been applied to study the energetics of proton translocation in cytochrome oxidase. Redox potentials of the metal centers and the tyrosyl radical have been computed, as well as pK_a values of important groups along the translocation path. Models with more than 100 atoms have been used with geometries fully optimized in the presence of a dielectric continuum to represent the surrounding enzyme. The models are built from the bovine X-ray structure (2OCC), which does not contain water molecules. The main result obtained is that for these models the pK_a values of propionate A of heme a_3 are actually larger than those of the oxo and hydroxyl groups of the binuclear center, even after an electron has been transferred to heme a_3 from heme a . The consequence of this rather surprising finding is that a proton coming from the inside of the membrane will actually thermodynamically prefer to go to the propionate for further pumping rather than go to the binuclear center for consumption in the oxygen chemistry. Full energetic cycles are constructed for both the case without and the case with a proton gradient across the membrane.

I. Introduction

Cytochrome oxidase is the terminal enzyme in the respiratory chain. It catalyzes the reduction of dioxygen to water and couples this reaction to the translocation of protons across the mitochondrial (or bacterial) membrane. The translocated protons drive the synthesis of ATP, where the energy of food consumption and respiration is stored. The X-ray structure of cytochrome oxidase was solved a few years ago for both a bacterial¹ and a mammalian species,² and recently for a second bacteria.³ There are four redox centers in the enzyme: Cu_A and heme a , which function as electron transport cofactors, and Cu_B and heme a_3 , which form the binuclear center (bnc), the active site for dioxygen reduction (see Figure 1).

The reaction catalyzed by cytochrome oxidase is



For each O_2 molecule, eight protons are taken up from the inside, and four of these protons are pumped to the outside across the membrane.⁴ The electron-transfer pathway starts at Cu_A , which receives an electron from a cytochrome c on the outside of the membrane. From Cu_A the electron goes to heme a and then on to the binuclear center. Protons are transferred from the inside of the membrane along two different pathways, the D and the K channels. It is believed that, at most, one of the eight protons follows the K pathway, which leads to the binuclear center.⁵ All four protons pumped, and at least three of the protons consumed in the dioxygen reduction thus follow the D channel.

Dioxygen reduction in cytochrome oxidase occurs in four steps, one for each electron being transferred to the binuclear center. A large amount of spectroscopic information has been gathered over the past decades characterizing the intermediates of the binuclear center appearing during this cycle.^{7–9} A brief overview of the catalytic cycle of cytochrome oxidase is shown in Figure 2. References to these intermediates will be made in the discussion below. Starting with the reduced form of the

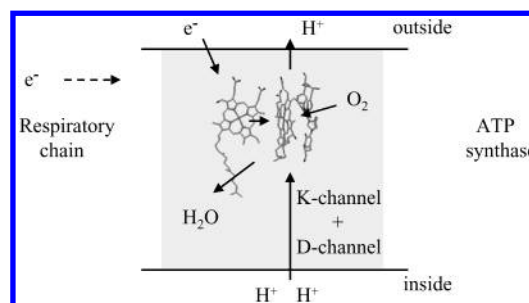


Figure 1. Schematic structure of cytochrome oxidase.

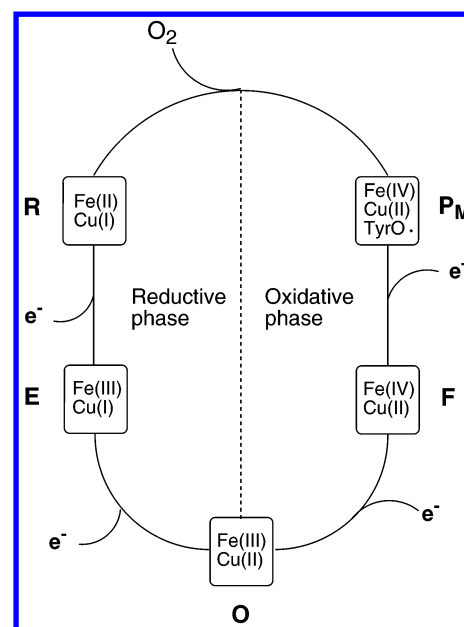


Figure 2. Catalytic cycle of cytochrome oxidase.

enzyme, intermediate **R**, the oxidation states of the binuclear center are Fe(II)–Cu(I). When O_2 becomes bound, intermediate

A is formed. Cleaving dioxygen leads to intermediate P_M , which has the oxidation states Fe(IV)–Cu(II), and presumably a tyrosyl radical. With an additional electron the intermediate is termed P_R . Intermediate **F** is formed with one additional proton at the binuclear center and the same oxidation states as P_R . With one additional electron transferred and also one more proton, the **O** state is formed. These steps constitute the oxidative phase. In the reductive phase, the two subsequent electrons are transferred, and the active site is reduced back to the **R** state. The intermediate in which only one electron has been transferred is termed **E**. A major controversy exists concerning the number of protons being translocated in each part of this cycle.⁶ For a long time, it was generally agreed that all four protons are translocated during the oxidative phase, two between P_M and **F**, and two between **F** and **O**.¹⁰ More recently this conclusion has been questioned, and it was proposed that only one proton is translocated between **F** and **O**.¹¹ The fourth proton should then be translocated during the reductive phase.¹² It has also been suggested that, even though only three protons are translocated in the oxidative phase, the energy needed for translocation of all four protons is made available during this phase.¹³ The question of the number of protons being translocated in each step is still not settled, but this is not a key issue of the present study. Instead, the focus is here on the general question of how oxygen reduction is coupled to proton translocation. It has been proposed that the propionates of heme a_3 play an important role in the proton translocation,¹⁴ and in the present study it will be assumed that the translocated protons will pass via the heme a_3 propionates.

There are two leading suggestions for the proton pumping mechanism in cytochrome oxidase. The first one is the so-called histidine cycle of Wikström and co-workers.^{15–17} A key feature of this mechanism is that a gate is present that passes the protons for either pumping or consumption (oxygen reduction). Such a gate is suggested to be needed to prevent the protons from going directly from the inside to the strongly exergonic O_2 reduction chemistry, and instead be directed toward the endergonic pumping. One cycle of this mechanism in the oxidative phase can be briefly described as follows. An electron is first transferred from heme a to the binuclear center. This leads to a large driving force for proton transfer to the binuclear center from the inside of the membrane. However, these protons cannot reach the binuclear center but are hindered on their way by the conserved His291 ligand of Cu_B , which is initially in an imidazolate state (Im^-). When two protons have reached this histidine, leading to an imidazolium group (ImH_2^+), this group can swing out from the Cu_B center toward the propionates. This means that the proton gate is open, resulting in proton flow from the inside into the binuclear center where the charge is annihilated and the chemistry completed. As a consequence, the imidazolium group is destabilized, and protons are released to the outside. When the histidine returns as an imidazolate, the cycle is closed. The net result is thus a translocation of two protons across the membrane and a reduction of the binuclear center. In this mechanism, all the energy used for proton translocation is generated in the oxidative phase. It should be added that it is also possible to translocate only one proton with this mechanism. A detailed scheme assigning all intermediates observed, as well as the motion of all translocated and consumed protons, has been suggested using this mechanism for translocation.

The second leading mechanism of proton translocation in cytochrome oxidase is that proposed by Michel and co-workers, based on electrostatics.^{11,18} In this model, each of the four

reductions of heme a during the catalytic cycle is coupled to the uptake of one proton. These protons (not more than two at a time) are temporarily stored in the regions of the heme a and heme a_3 propionates and are driven to the outside by electrostatic repulsion from protons entering the binuclear center. A detailed scheme showing the proton and electron transfers, involving all intermediates observed, has been suggested. An important point of this scheme in comparison to the histidine cycle is that the reductive phase plays a bigger role in proton translocation. Also, heme a is more important. The question of how the protons are gated is not clearly addressed in this mechanism.⁶ For example, if the protons on the propionates are not prevented from moving to the binuclear center as the electron moves to this site, it appears that a large amount of available energy could be dissipated.

In the present density functional study, the mechanism for translocation in cytochrome oxidase is addressed once again. Proton affinities (corresponding to pK_a values) and electron affinities (corresponding to reduction potentials) are calculated for key elements of the binuclear center and the propionates with and without additional electrons and protons at the active site. A comparison of these numbers leads to suggestions for how the active site should be organized to allow proton translocation. One of the questions addressed is whether a gate at the entrance of the binuclear center is needed. Is there a reason to prevent the protons from entering the binuclear center at any stage? If not, how can the protons be directed toward a costly translocation rather than toward the exergonic protonation of the oxygen ligands?

II. Computational Details

The calculations were performed in two steps. For each structure considered, a geometry optimization was performed using the hybrid density functional B3LYP method in its unrestricted version.¹⁹ In the geometry optimization, certain atoms were frozen from their X-ray positions, and those atoms are marked with asterisks in the figures displaying the models used. In this first step, standard double- ζ basis sets were used for all light elements. For iron and copper, nonrelativistic effective core potentials (ECPs) were used.²⁰ The valence basis set used in connection with this ECP is essentially of double- ζ quality (the *lacvp* basis set). Normally, geometry optimizations including a dielectric continuum are not needed, since dielectric effects are usually found to be quite small. However, this is not so for some of the systems discussed here, where large charge separations appear, and the geometry optimizations were therefore performed for all systems with the dielectric medium included. The dielectric constant of the homogeneous dielectric medium was set equal to 4.0, in line with previous experience.²¹ The probe radius was set to 1.40 Å, corresponding to the water molecule. To test the sensitivity of the results to the choice of dielectric constant, a few calculations were done with a value of 80.0 corresponding to the one in water. The results showed that the computed proton affinities changed by about 5 kcal/mol, while the relative proton affinities changed by about 1 kcal/mol.

In the second step, the B3LYP energy was evaluated at the optimized geometries using a larger basis set, the *lacv3p** basis set, which is of triple- ζ quality and uses a single set of polarization functions on each heavy atom. The basis set extension effect was obtained in gas-phase calculations. All the calculations were carried out using the Jaguar program.²² No

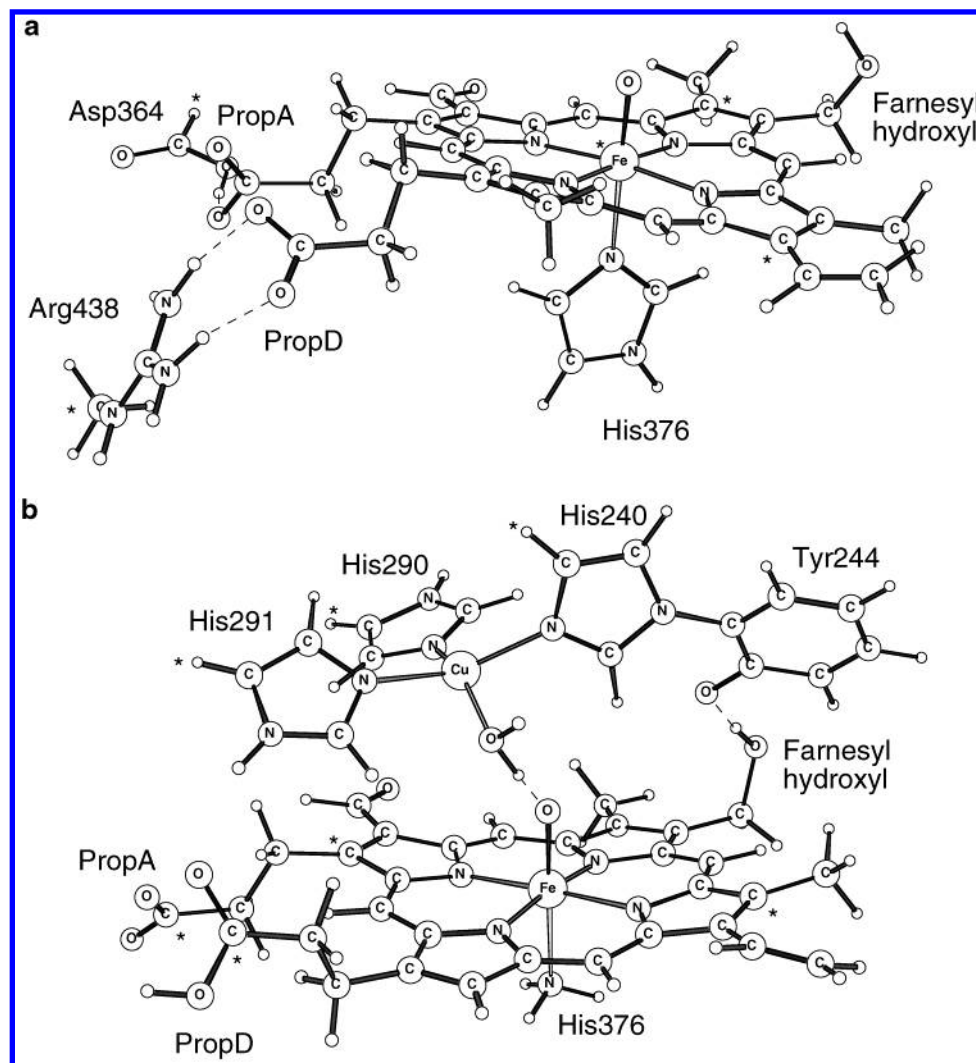


Figure 3. Two models used to study proton and electron affinities in the binuclear center of cytochrome oxidase

Hessians were computed, since zero-point and temperature effects are expected to be small on most of the energy differences of interest here and, for the large models used, Hessian calculations are extremely time-consuming. In the few cases where entropy effects are expected to be important, the procedure used is discussed in the text below.

The inherent accuracy of the B3LYP functional has been estimated using the extended G3 benchmark set,²³ consisting of enthalpies of formation, ionization potentials, electron affinities, and proton affinities for first- and second-row molecules. This test has 376 entries, and the B3LYP functional obtains an average error of 4.3 kcal/mol.²³ Excluding 75 enthalpies of formation for large molecules, involving the formation of a large number of new bonds, which should not be relevant for the present study, an error of 3.3 kcal/mol is obtained for the B3LYP functional (301 entries). For transition metals, there are no benchmarks due to the lack of accurate experimental numbers, but indications from normal metal–ligand bond strengths are that the errors are slightly larger, 3–5 kcal/mol.²⁴ For further information on the present type of calculations, see recent reviews.^{25–27}

III. Results and Discussion

In the present study, proton affinities (PAs) and electron affinities (EAs) in the active site of cytochrome oxidase have been calculated. Two different models were treated, both built

on the bovine X-ray structure (2OCC²), which does not contain any water molecules in this region. In the first model, only heme a_3 is considered (see Figure 3a). The full porphyrin is included, except the long farnesyl side chain, which is replaced by a hydroxylated methyl group and referred to as the farnesyl hydroxyl group in the figure. For the two propionates, the most important hydrogen-bonding residues from the surrounding protein are also included. Arg438, which is hydrogen bonding to the propionate on the D-ring, is modeled by a protonated formamidine, and Asp364, which is hydrogen bonding to the propionate on the A-ring, is modeled by a formic acid. The axial His376 is modeled by an imidazole. In the second model, both heme a_3 and Cu_B are included (see Figure 3b). A somewhat simpler model of heme a_3 is used as compared to the first model. The axial histidine is modeled by ammonia, and the hydrogen-bonding residues of the propionates are left out. Instead, the propionate on the D-ring is modeled as protonated, representing the interaction with the positively charged arginine, and the propionate on the A-ring interacting with the neutral aspartic acid is modeled as unprotonated. The effect of leaving out the hydrogen-bonding residues was checked for the heme a_3 model, and it was found that the proton affinity of the A-ring propionate was increased by 3.3 kcal/mol. Therefore, in all results for the binuclear model reported below, the calculated proton affinity of the A-ring has been decreased by 3.3 kcal/mol to account for the omitted hydrogen bonding. For Cu_B , the three histidine

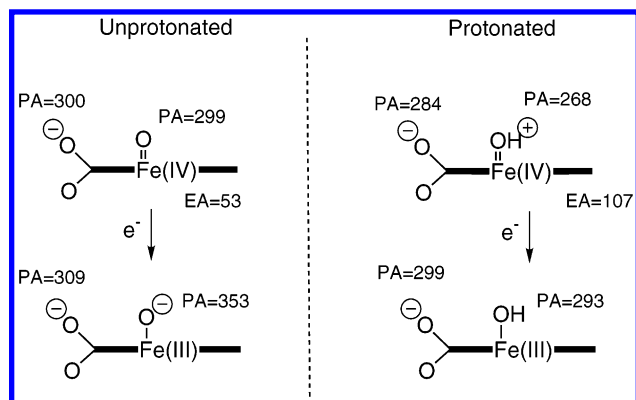


Figure 4. Calculated proton and electron affinities, in kcal/mol, for the heme a_3 model.

ligands are modeled as imidazoles, while the covalently linked tyrosine is modeled as a phenol.

The investigation discussed in the first subsection below concerns the proton affinities of heme a_3 , comparing protonation of the iron-bound oxygen with protonation of the propionates. Since the two propionates have rather different surroundings, their proton affinities are also rather different. The propionate proton affinity discussed in this study is that of propA (see Figure 3), which is the largest one. The proton affinities discussed in the first subsection below are those calculated for the Fe(IV) state, corresponding, for example, to the **F** intermediate in the catalytic cycle, and for the Fe(III) state, corresponding to the situation after an additional electron has been transferred to heme a_3 . Both models in Figure 3 were used in this investigation. In the second subsection, the calculated electron and proton affinities of heme a are discussed. The model calculations presented in the first subsection led to an idea for proton pumping which is pursued in the third subsection, describing proton and electron flow for both the oxidative and reductive parts of the catalytic cycle in cytochrome oxidase.

A. An Important Proton Effect at the Binuclear Center.

A key problem for the mechanism of proton pumping in cytochrome oxidase is whether a gate is needed to prevent premature protonation of the binuclear center. To study this problem, the model of heme a_3 shown in Figure 3a was first used. The results are summarized in Figure 4.

In the first calculations, the proton affinities of the oxo group and the heme propionate were determined with iron in oxidation state Fe(IV). The reason to start the analysis here is that this state corresponds, for example, to the quite well-defined **F** state, and it is also generally agreed that a proton is being translocated in the **F**-to-**O** transition. Using the model in Figure 3a, quite similar proton affinities of 299 kcal/mol for the iron-oxo group and 300 kcal/mol for the propionate were found, as can be seen on the left in Figure 4. Next, an electron is transferred to the heme. Not surprisingly, this leads to a substantially increased proton affinity of the oxo group by 54 kcal/mol, to 353 kcal/mol. The effect on the propionate is much smaller, as expected, with an increase of only 9 kcal/mol, to 309 kcal/mol. In the context of cytochrome oxidase, this can be interpreted to show that after the electron has been transferred to the binuclear center, the proton affinity is much larger for the oxo group than for the propionate. It seems clear that if a proton is allowed to flow freely into the active site, this will just lead to a protonation of the oxo group, and a large amount of energy will be dissipated. No proton will be transferred to the propionate for further pumping. At this stage, the picture is as expected.

To change the above picture to one of proton pumping, something has to be done to the active site. One possibility

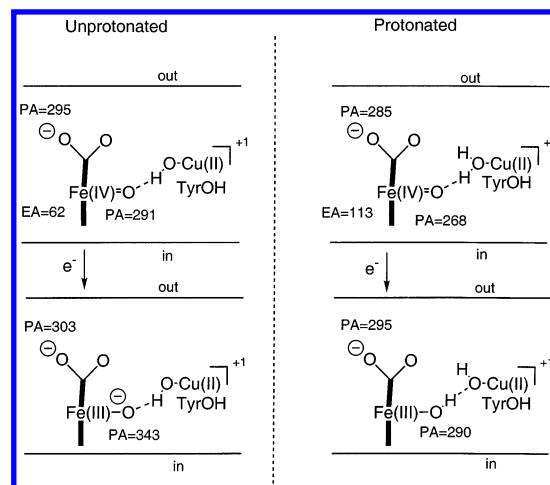


Figure 5. Calculated proton and electron affinities, in kcal/mol, using the binuclear model.

would be the histidine cycle mechanism, where His291 is suggested to block proton flow into the binuclear center until pumping has been achieved. Another, much simpler possibility is investigated for the present model systems, and this is to assume that the oxo group is protonated before the reduction of the binuclear center occurs. It is clear that this will strongly affect the computed proton affinities. The result from the calculations, shown on the right in Figure 4, is that the proton affinity of the iron-bound oxygen (now a hydroxyl group) before the electron enters the binuclear center is reduced by 31 kcal/mol, to a value of 268 kcal/mol. The propionate PA is only reduced by 16 kcal/mol, to 284 kcal/mol. The effect of prior protonation is consequently that the proton affinity is substantially larger by 16 kcal/mol at the propionate than at the binuclear center oxygen. However, the most interesting effect is that the proton affinity continues to be largest at the propionate, even after an electron has been transferred to the binuclear center. When the electron is transferred, the PA of the Fe(III)-OH group is increased by 25 kcal/mol, which is more than the increase by 15 kcal/mol of the propionate, but not enough to make the PA of the Fe(III)-OH group larger than that of the propionate. If this was a good model of the binuclear center, the first proton that comes in (either from PropA of heme a or from the inside of the membrane) after the electron has been transferred to the binuclear center would therefore choose to go to the propionates for further pumping rather than to go to the binuclear center and be consumed. The problem of unwanted energy dissipation at this stage would thus be solved without the need to block the pathway to the binuclear center. The question is only if the simple chemical model used is representative of the actual binuclear center. This will be discussed next using the more realistic model in Figure 3b.

It is clear that a proton must be involved in the O-O bond cleavage step.^{11,16,28,29} This leads to the presence of one proton at the binuclear center already in the **P_M** state, which supports the picture with an extra proton given above. This proton could come either from the cross-linked Tyr244 or from some other place. The possibility that an additional proton is present at the binuclear center prior to the O-O bond cleavage has been suggested in recent papers,^{28,29} in which model calculations showed that the barrier for O-O bond cleavage is much too high without an added proton in intermediate **A**. Without this additional proton, the binuclear center would be described as shown on the left in Figure 5, at the level of the Fe(IV) oxidation state. Before the electron has been transferred to the binuclear center, the PA of the Fe(IV)-oxo group is 291 kcal/mol, and

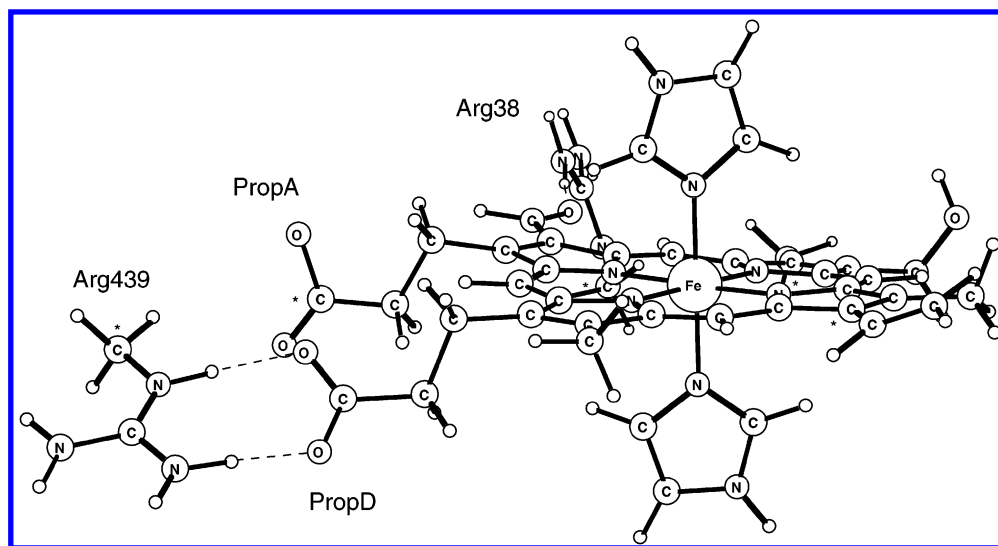


Figure 6. Model used to study electron and proton affinities of heme a.

that of the propionate is 295 kcal/mol. After an electron has been transferred to this state, the calculated proton affinities are 343 kcal/mol for the iron–oxo group and 303 kcal/mol for the propionate using the binuclear model of Figure 3b. These results are thus qualitatively similar to those of the pure heme a_3 model of Figure 3a for the case without an added proton (on the left in Figure 4). The conclusion is that, if there is no gate to prevent the protons from getting into the active site, there will be no pumping. On the other hand, the previous model calculations for the O–O bond cleavage^{28,29} and experiments^{11,16} suggest that the protonation state of the binuclear center at the level of the Fe(IV) oxidation state is rather as shown on the right in Figure 5. The additional proton is placed on the hydroxyl group on copper, forming a water molecule. The proton affinity of the oxo group now decreases by 23 kcal/mol, to 268 kcal/mol, while that on the propionate decreases by only 10 kcal/mol, to 285 kcal/mol. At this stage, the PA of the propionate is thus substantially larger by 17 kcal/mol than that of the oxo group. When the electron is transferred to the binuclear center, the PA of the Fe(III)–OH group increases by 22 kcal/mol, and that of the propionate increases by 10 kcal/mol. Again, as for the heme a_3 model, this leads to the interesting result that the PA of the propionate, 295 kcal/mol, is larger than that of the Fe(III)–OH group of 290 kcal/mol. *This means that the proton clearly prefers to go to the propionates for further pumping rather than being consumed at the binuclear center.* With this type of protonation state, there is thus no need for a gate at the binuclear center at this stage.

The electron affinities (EAs) have also been computed for the models in Figure 3, and the results are shown in Figures 4 and 5. The results of the two models are quite similar, just as for the PAs. For the binuclear model in Figure 3b, the EA of heme a_3 is 62 kcal/mol without and 113 kcal/mol with the additional proton. For the model in Figure 3a, the corresponding results are 53 and 107 kcal/mol. From the results described in the next section below, it will be clear that an EA of 50–60 kcal/mol is far from enough to draw an electron from heme a. An EA of about 110 kcal/mol is much more in line with what is required. These results therefore strongly suggest that the protonation state of the binuclear center is as shown on the right in Figures 4 and 5 rather than that on the left, thus supporting a picture with an additional proton present at the binuclear center.

A major part of the effects described above are clearly electrostatic in nature, but there are also chemical effects

requiring the present DFT treatment rather than a simpler, purely molecular mechanical treatment. For example, adding a proton to the heme a_3 –oxo group in the binuclear model (see Figure 5) decreases the PA of the oxo group by 23 kcal/mol and that of the propionate by 10 kcal/mol. If an electron is first added to heme a_3 , the effects are instead 53 and 8 kcal/mol, respectively. With a pure electrostatic effect of the extra proton, these changes should have been the same before and after the electron is added. Similarly, adding an electron to the model without the added proton increases the PA of the heme a_3 –oxo group by 52 kcal/mol and that of the propionate by only 8 kcal/mol. Adding the electron to the model with the added proton increases the PA of the heme a_3 –oxo group by 22 kcal/mol and that of the propionate by 10 kcal/mol. Where a model with just point charges would have given a similar size of the changes in these cases, the actual values calculated by B3LYP differ quite substantially, and the reason for this is that the added electrons and protons actually are involved in chemical processes.

Another interesting value that can be obtained from the calculations is the sum of the EA and PA. For the binuclear model without the added proton, this value becomes 405 (= 62 + 343) kcal/mol, and with the added proton it is 403 (= 113 + 290) kcal/mol. In both cases, an FeO–H bond has been formed, and this bond strength is hardly affected by the surrounding charge distribution, in contrast to the PAs and EAs.

B. The Electron and Proton Affinities of Heme a. The model used for heme a is shown in Figure 6. The model is similar to that used for heme a_3 in Figure 3a. The full porphyrin is retained, except for the long farnesyl side chain, which is replaced by a hydroxylated methyl group. The most important hydrogen-bonding residues from the surrounding protein, two arginines, are also included, together with the axial histidine ligands. The histidines are modeled as imidazoles and the arginines as formamidines. Since the negatively charged propionate A (PropA) has no counter charge from the protein, two different protonation states of heme a are considered, i.e., with and without a proton on propionate A. The calculated EA without a proton on the propionate is only 91 kcal/mol. As seen above, and further below, this value is not enough in comparison to the EA of the different realistic models of heme a_3 , which are in the range 103–113 kcal/mol. The calculated EA of heme a with a protonated PropA of 104 kcal/mol is much more in line with that for heme a_3 . It is therefore concluded that, at the

stage of electron transfer from heme a to heme a₃, PropA of heme a is protonated.

The proton affinity of PropA of heme a is also important for the proton translocation mechanism discussed below. The calculated PA for heme a in the Fe(II) reduced state is 301 kcal/mol, and that in the Fe(III) oxidized state is 288 kcal/mol. One conclusion drawn from these values is that, as heme a becomes reduced, a proton must be present on PropA; otherwise, the electron affinity (reduction potential) of heme a will be much too low (see above). There are two possibilities: either this proton is always there, or it is transferred from the inside of the membrane to PropA as heme a becomes reduced.¹¹ The present calculations are not accurate enough to conclude which of these possibilities is most likely. However, since there are experimental indications³⁰ that there is no uptake of protons as heme a becomes reduced, at least without membrane potential, it will be assumed in the following that the proton is always present on PropA of heme a.

C. Suggested Proton and Electron Flow in Cytochrome Oxidase. In section III.A, it was shown that it is possible to arrange the protonation of the binuclear center in a way that leads to a situation where the protons energetically prefer to go to the propionate rather than to the binuclear center. In this section, all steps in the oxidative and reductive phases of the catalytic cycle will be described for the protonation state suggested above using the binuclear model of Figure 3b. This description will start with the **F**-to-**O** transition (see Figure 2), since this step follows most naturally from the results of the preceding sections. The other transitions will be described after that.

To simplify comparisons to experiments, in this section the EAs will be given as redox potentials and the PAs as pK_a values. To transform the computed EAs to redox potentials, 4.1 eV is subtracted, and to transform the PAs to pK_a values, pH 7 is assumed to correspond to a PA of 289 kcal/mol. The value of 4.1 eV is chosen to put the redox potential for heme a at 0.40 V, which is within the experimental range of values. A strict transformation would use either the standard hydrogen gas electrode of 4.43 eV or the standard calomel electrode of 4.19 eV. Using 4.43 eV, the calculated redox potential for heme a becomes 0.08 V, and using 4.19 eV it becomes 0.32 V, indicating that the error in the calculations is quite small. The assumption that pH 7 corresponds to 289 kcal/mol is less well defined but is taken to make the best match of the present calculations against experiments for cytochrome oxidase (see further in the concluding section IV). It should be noted that the value chosen is a constant, which will not affect relative pK_a 's.

The F-to-O Transition. The starting point for this transition is the **F** intermediate, which has an Fe(IV)–oxo group and a water molecule bound to Cu(II). It corresponds to the situation where an additional proton has been placed at the binuclear center, following the nomenclature from above. The results for the **F**-to-**O** transition are shown in Figure 7. The first step of this transition is that an electron is transferred from heme a to heme a₃. The calculated redox potential for heme a₃ is 0.82 V, which means that electron transfer from heme a should be exergonic by 9.7 kcal/mol, since the redox potential of heme a is 0.40 V, with a proton at PropA (see section III.B). It can be noted that, without the additional proton at the binuclear center, the redox potential is only –1.41 V (corresponding to 62 kcal/mol; see Figure 5), which is far from enough to pull the electron from heme a. The redox potential of heme a without the additional proton on PropA is only –0.15 V. If this value is

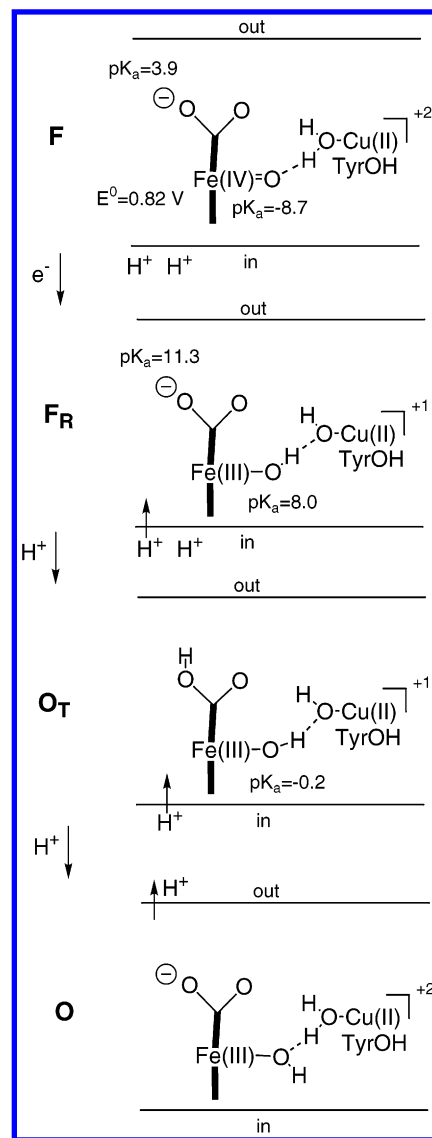


Figure 7. Proton and electron flow in the **F**-to-**O** transition using the binuclear model.

used, the exergonicity for electron transfer to heme a₃ would be 22 kcal/mol, which is too much. The calculated pK_a 's of the **F** intermediate are –8.7 for the heme–oxo group and 3.9 for the propionate. The pK_a of the propionate is thus substantially larger by 12.6 units at this stage. It is clear that none of these pK_a 's is big enough to pull a proton from the inside of the membrane with pH 7. The pK_a of PropA of heme a₃ is not quite enough to draw a proton from PropA of heme a either, since the pK_a of this group is 6.3 in the oxidized state (see above).

After the electron transfer from heme a to heme a₃, intermediate **F_R** is reached, named to correspond to intermediate **P_R**, which is an observable state. The pK_a 's obviously increase on going from **F** to **F_R**, by 16.7 units, to 8.0, for the heme–oxo group and by 7.4 units, to 11.3, for the propionate. It is interesting to note that the pK_a of the propionate is larger than that of the heme–oxo group at this stage.

In intermediate **F_R**, the pK_a of the propionate of heme a₃ is now large enough that a proton is transferred exergonically by 5.9 kcal/mol from the inside. With the calculated pK_a 's for the **F_R** intermediate, the proton will automatically go to the propionate, not to the binuclear center, and no proton gate is needed at this stage. It is assumed that this step will have time to form at thermodynamical equilibrium. This means that if the

proton happens to go to the binuclear center, it will have time to find the better position at the propionate. As for all other mechanisms suggested so far, it is also assumed here that proton transfer from the outside of the membrane is substantially slower.

After the proton transfer to the propionate has occurred, intermediate **O_T** is formed. The **F_R**-to-**O_T** transition is thus a fast exergonic process in thermodynamical equilibrium. Only the **O_T**-to-**O** step now remains in this transition. In this step, a proton should be transferred from the inside to the binuclear center along the D channel. There may appear to be a problem connected with this transfer, since the calculated pK_a of the Fe(III)–OH group is now quite low. As the proton was transferred to the propionate in the preceding **F_R**-to-**O_T** transition, the pK_a of the Fe(III)–OH group decreased from 8.0 to –0.2 units as a result of a direct electrostatic repulsion. However, by moving the proton on the propionate to the outside, the pK_a of the Fe(III)–OH group should be back at 8.0 units, which thus helps the proton to get into the binuclear center. This process can also be described by saying that the proton moving along the D pathway repels the proton on the propionate to the outside. This part of the present mechanism is therefore similar to the corresponding part suggested by Michel,¹¹ for example. Assuming no membrane potential (pH 7 on the outside), this step will be endergonic by 4.5 kcal/mol. This step, like other endergonic steps, is instead driven by the exergonicity of a later step, such as the electron transfer from heme a or proton transfer to the propionate (see further below). This part concludes the suggested **F**-to-**O** transition.

The P-to-F Transition. The transition from **P** to **F** is suggested to be somewhat more complicated than that from **F** to **O** described above. The results are shown in Figure 8. Directly after the O–O bond cleavage, intermediate **P_M** is formed with a structure as indicated in the figure. The oxidation states of the metals are Fe(IV) and Cu(II). As suggested experimentally,³¹ Tyr244 is also oxidized and forms a neutral tyrosyl radical. Since the pK_a of PropA of heme *a*₃ is as high as 11.5, a proton should already have moved from the inside to PropA of heme *a*₃ in the preceding reductive step (**E** to **R**, see below). This means that both propionates, on heme *a* and heme *a*₃, are already protonated before the electron has reached heme *a*₃. The calculated pK_a of the heme *a*₃–oxo group is –0.3 and does not draw a proton from the inside at this stage.

The first step in this transition is that an electron comes in from heme *a* to the tyrosyl radical, forming intermediate **P_R**. The calculated redox potential of the tyrosyl radical is 0.54 V, suggesting that the electron transfer should be exergonic by 3.2 kcal/mol, since the redox potential of heme *a* is 0.40 V. The calculated redox potential of heme *a*₃ is much smaller, with the value –0.85 V.

At this stage, **P_R**, a proton is suggested to be transferred to the tyrosinate from the inside, leading to intermediate **F_{T1}**. The calculated pK_a of the tyrosinate is 12.0 units. Just as in the case of the **F**-to-**O** transition, the proton on the propionate is repelled to the outside as the proton going along the D channel moves from the inside toward the tyrosinate. This step is exergonic by 1.5 kcal/mol.

After the proton has been expelled to the outside, the pK_a of the propionate is now quite high, at 10.9 units. This leads to another proton transfer from the inside to the propionate, forming intermediate **F_{T2}** in a step that is exergonic by 5.4 kcal/mol.

Intermediate **F_{T2}** has a very low pK_a on the Fe(IV)–oxo group of 2.3 units. Since a proton still needs to get into the active site

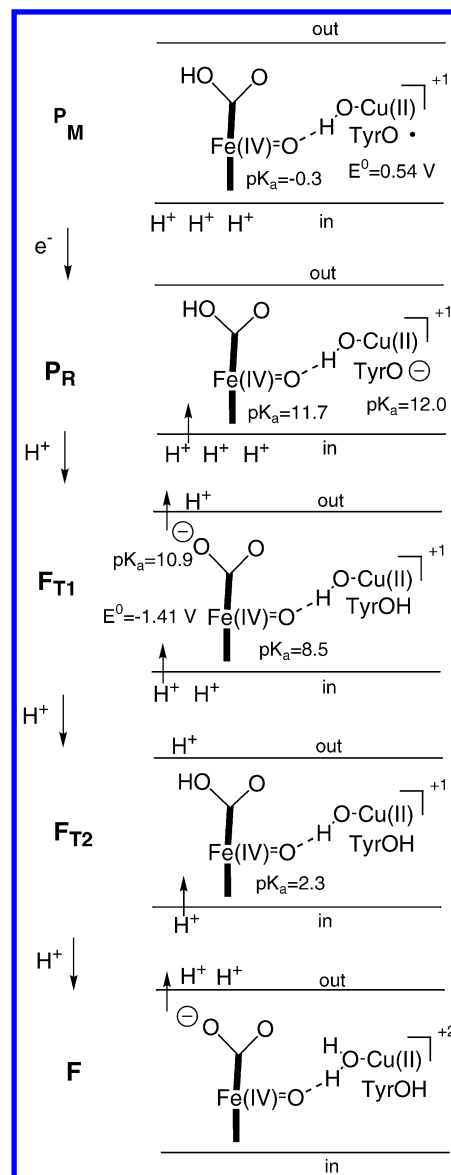


Figure 8. Proton and electron flow in the **P**-to-**F** transition using the binuclear model.

to allow the next electron transfer, it is suggested that the propionate proton moves to the outside, which increases the pK_a of the binuclear center to 8.5 units. The proton will then be transferred from the inside to the binuclear center to conclude the **P**-to-**F** transition. These proton transfers, from the propionate to the outside and from the inside to the binuclear center, can also occur concertedly, of course. The process can also be described as one where the proton from the inside going to the binuclear center along the D channel repels the proton on the propionate so that it goes to the outside. The step is endergonic by 3.3 kcal/mol, assuming no membrane potential.

The O-to-E Transition. The transition from **O** to **E** is the first part of the reductive phase. This transition is suggested to be quite similar to that from **F** to **O** (see Figure 9). One difference is that the electron coming from heme *a* is not suggested to go to iron but rather to copper. The calculated redox potential of Cu(II) in intermediate **O** is 0.76 V, leading to an exergonicity of 8.3 kcal/mol for this electron transfer. In the calculated redox potential, a correction for entropy effects is included, increasing the value by 0.26 V (6 kcal/mol). This is done since, during the reduction, the water molecule becomes very loosely bound to copper, with the Cu–O bond distance increasing from 1.97

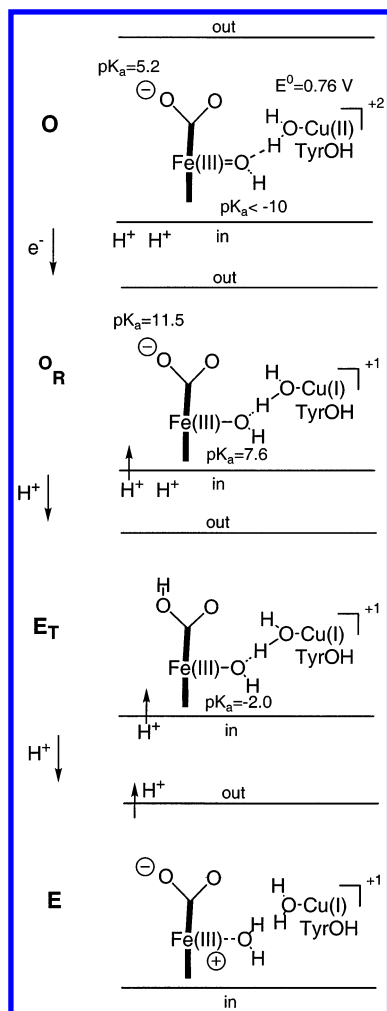


Figure 9. Proton and electron flow in the **O**-to-**E** transition using the binuclear model.

Å in **O** to 2.28 Å in **O_R**. A similar effect was previously found in a study of the O–O bond cleavage step, going from compound **A** with a loosely bound water molecule to **P_M** with a hydroxyl group on copper.²⁹ In that case, the calculations, using much smaller models for the binuclear center, for which Hessian calculations can more easily be performed, gave an entropy effect of 6 kcal/mol on the activation energy, which is also in agreement with experimental observations for the temperature dependence of the reaction rate.³² Therefore, a similar correction of 6 kcal/mol was introduced here.

After electron transfer, intermediate **O_R** is formed. This intermediate has a pK_a of the propionate of 11.5 units, similar to those of the previous transitions. This leads to an exergonic proton transfer from the inside to the propionate of 6.2 kcal/mol, leading to intermediate **E_T**.

The calculated pK_a of the binuclear center for intermediate **E_T** is, as in the other transitions, quite low, –2.0 units. After the proton on the propionate is expelled to the outside, the value is 7.6 units. In this value, an entropy correction of 6 kcal/mol is included, since a water molecule rather loosely coordinated to iron is formed (compare the discussion on the reduction of copper above). In fact, the structural changes at the iron center occur in two steps, first when the water molecule is formed, and then also when the iron is reduced. Since the changes are somewhat larger in the first step, it was decided to make the whole entropy correction here. A proton is now transferred from the inside to the binuclear center, and as before, a proton is also expelled to the outside from the propionate in this process,

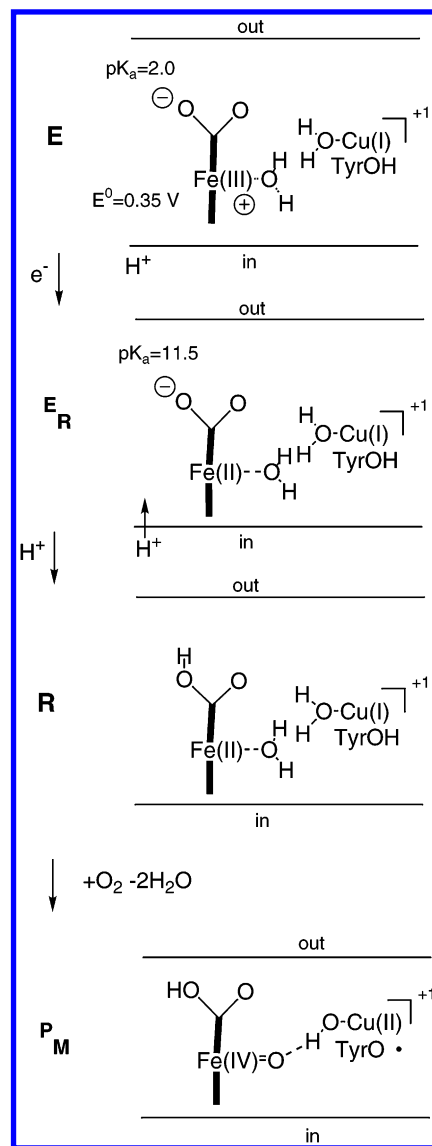


Figure 10. Proton and electron flow in the **E**-to-**R** transition using the binuclear model.

which concludes the **O**-to-**E** transition. This step is endergonic by 5.4 kcal/mol without membrane potential.

The E-to-R Transition. The transition from **E** to **R** is the final part of the reductive phase (see Figure 10). The redox potential of Fe(III) in intermediate **O** is calculated to be 0.35 V. This means that the electron transfer from heme a will be slightly endergonic by 1.2 kcal/mol.

The pK_a of the propionate in **E_R** is 11.5 units, which is quite similar to the situation in the previous transitions. This means that there will be a 6.2 kcal/mol exergonic proton transfer from the inside to the propionate forming intermediate **R**. Since there is no place for another proton at the binuclear center, the only step remaining to close the catalytic cycle of cytochrome oxidase is the O₂ cleavage process, leading to intermediate **P_M**, where the present description started.

The only mechanism used here to move protons to the outside expels these protons from the propionate as a proton is transferred along the D channel to the binuclear center. Since only four protons are transferred from the inside to the binuclear center, and four protons are known to be translocated in one cycle, a proton has to be expelled to the outside every time this happens. For the same reason, there will be no proton translocation in the **E**-to-**R** transition.

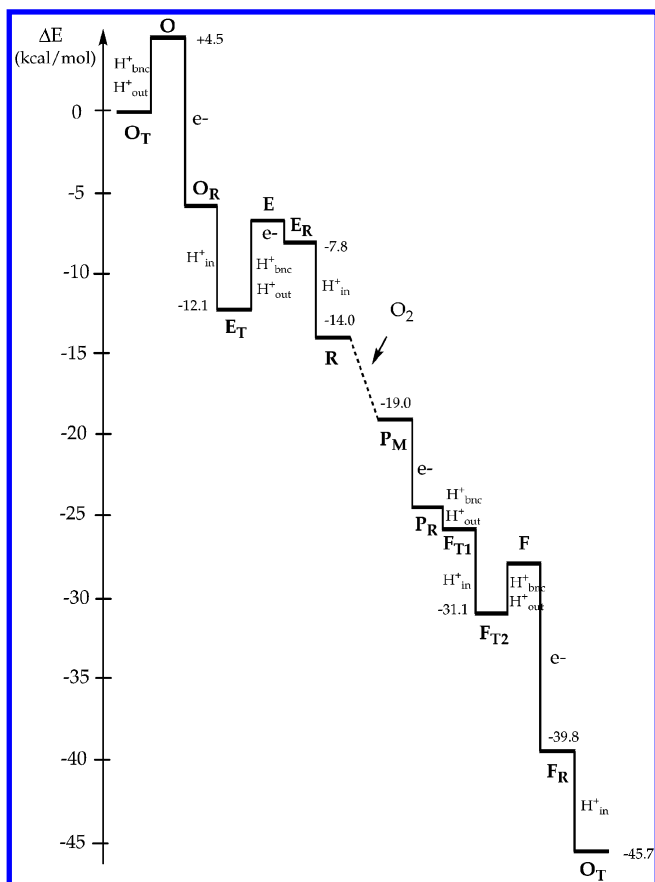


Figure 11. Potential energy surface for an entire cycle of cytochrome oxidase in the case without membrane potential.

IV. Summary and Conclusions

In the present study, pK_a values and redox potentials for the active site of cytochrome oxidase have been calculated. A major finding is that the pK_a value of PropA of heme a_3 can actually be larger than that at the binuclear center (bnc), even when an electron has been transferred to the binuclear center. This situation is reached if an additional proton is placed at the binuclear center. The proton could come from the cross-linked Tyr244 or from some other place. The large pK_a value of PropA has the effect that a proton from the inside actually prefers to go to PropA for further pumping rather than to be consumed in the dioxygen chemistry at the binuclear center. This should be a major part of the gating mechanism which is needed for proton pumping.

The energetics of the proton and electron flow, as discussed in the preceding sections, can be summarized in the diagram shown in Figure 11. This diagram is drawn with the assumption that there is no membrane potential. To simplify comparison to experimental data, the energy gained from the electron transfer between cytochrome *c* and heme *a* is included in each electron-transfer step. It is assumed that the reduction potentials differ between cyt *c* and heme *a* by 0.1 V, corresponding to 2.3 kcal/mol. The O_2 bond cleavage step is assumed to be exergonic by 4 kcal/mol starting from P_M ,³³ and the **R**-to-**A** step is assumed to be exergonic by 1 kcal/mol. The PA corresponding to pH 7 also has to be chosen in some way, and it was decided to choose it to reasonably match the overall exergonicity of the entire cycle in Figure 11, which is known from experiments to be around 2 eV. This value is obtained from the reduction of O_2 to H_2O by cytochrome *c*. By choosing the PA of 289 kcal/mol to correspond to pH 7, the exergonicity actually calculated here becomes 45.7 kcal/mol. To conform with experimental conven-

tions, the diagram starts with the oxidized state. To make the entire diagram easier to follow, the description starts at the minimum O_T , which has a proton at PropA of heme a_3 . At O_T , a proton is transferred to the binuclear center, and the PropA proton is expelled in an endergonic step by 4.5 kcal/mol. As the proton has reached the binuclear center, an electron can be transferred from cyt *c* over heme *a* to Cu_B exergonically by 10.4 kcal/mol. The electron at Cu_B then allows a proton to go from the inside to PropA of heme a_3 exergonically by 6.2 kcal/mol to reach state E_T . The endergonic expulsion of the proton to the outside is thus driven by the two following exergonic steps. The E_T -to-**R** transition is less exergonic but otherwise quite similar to the O_T -to- E_T transition, and it also leads to the expulsion of one proton to the outside. In the scheme suggested here, the question of whether one or two protons are translocated in the reductive phase becomes a question of where the reductive phase starts. If it is considered to start in O_T , two protons are translocated, while if it starts at **O**, only one proton is translocated.

The O—O bond cleavage of dioxygen occurs between the reductive and oxidative phases and takes the system to state P_M . As pointed out above, the P_M -to- F_{T2} transition is somewhat different from the other transitions. In this case, the electron is transferred first, followed by the proton transfer to the binuclear center, in contrast to the other steps, where these transfers are reversed. This transition is quite exergonic by 12.1 kcal/mol. The final transition in the scheme in Figure 11 is the F_{T2} -to- O_T transition, which is the most exergonic transition with 14.6 kcal/mol. The main reason for this is a quite exergonic electron transfer of 11.8 kcal/mol.

It should be noted that the only mechanism for translocation used here is that a proton is expelled to the outside due to electrostatic repulsion from a proton moving from the inside to the binuclear center along the D channel. One consequence of this is that a proton transfer to the outside has to occur every time a proton moves into the binuclear center, even when it continues to the tyrosinate; otherwise, there would not be four protons translocated in the full cycle. The exergonic steps driving this pumping are the proton transfers from the inside to the propionates and the electron transfers from cyt *c* to the binuclear center.

The figure shows that most of the energy gain is obtained between **R** and O_T with 31.7 kcal/mol, while the steps between O_T and **R** give only 14.0 kcal/mol. It should be noted that no additional barriers of proton and electron transfers are added in the figure, apart from those involved in the endergonicities of some of the steps.

Finally, a diagram has been sketched for the situation where there is a membrane potential corresponding to 200 mV (4.6 kcal/mol; see Figure 12). The membrane potential affects all charge-transfer reactions over the membrane, thus giving a total reduction of the exergonicity of a full cycle by 36.8 kcal/mol. The effect of the membrane potential is included in each step of the catalytic cycle, assuming that the binuclear center (including prop A) is located at one-third of the distance from the outside to the inside. Thus, with the membrane potential, the full cycle is exergonic by 8.9 kcal/mol.

There are several ways in which the above diagrams can be modified. First, it must be remembered that the calculations can give errors which in some cases might be 5 kcal/mol for a relative pK_a or redox potential. There are also possibilities to modify the chemical model used. In the calculations discussed above, no water molecules were placed in the binuclear center at the stage when dioxygen is cleaved. From model calculations,

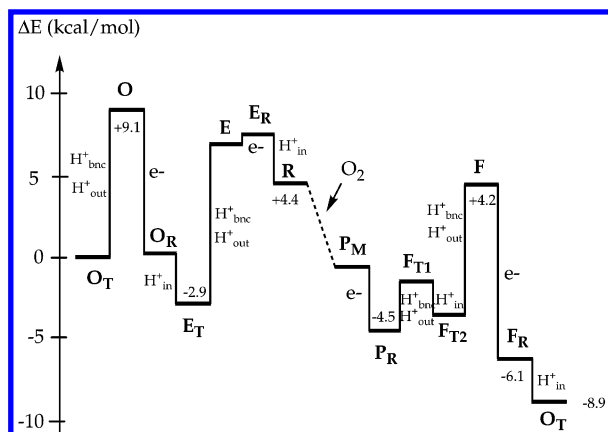


Figure 12. Potential energy surface for an entire cycle of cytochrome oxidase in the case with membrane potential.

it has been indicated that at least one, and probably two, water molecules are needed at the stage of O–O bond cleavage for protons to reach between tyrosine and dioxygen.^{28,29} If these water molecules are present, water has to be expelled from the binuclear center as the new water molecules are being produced in the dioxygen chemistry. This will clearly modify the calculated values in the different steps. Furthermore, water molecules in the propionate region, which are present in the recent bacterial X-ray structure,³ might modify the calculated pK_a values of the propionates. Apart from these obvious modifications of the calculated values, there are also different ways to use the computed values with only minor changes to construct different schemes. For example, in the present scheme, the tyrosinate is being protonated already in the P_R -to- F_{T1} step. Using almost the same computed values, it is possible to argue that this protonation should not occur until the E or R step. The effect of this modification has been studied recently for the F -to- O transition.³⁴ The conclusion at this stage is that a tyrosinate changes the energetics of the different steps somewhat but does not affect the main picture.

One of the main results obtained in the present study is that it is actually possible to have a situation where the protons from the inside energetically prefer to go to the propionates for pumping rather than to the binuclear center for consumption. However, it is important to note that gating is still needed at some points also in the present mechanism. First, for the pump to function, it has to be faster to take a proton from the inside to the propionates rather than from the outside. If this is arranged by having a high barrier for proton transfer between the outside and the propionates, it becomes difficult to design a situation where a transfer from the propionates to the outside has to be relatively fast in the proton expulsion steps. One reason for the difference in barrier heights in the two situations could be that the proton repulsion from the inside lifts the energy level of the protonated propionate to a point where the transfer of this proton to the outside is exergonic, but this can hardly be enough for the gating. A detailed study of the proton motion has to be performed to resolve this issue. A second need for a proton gate is to prevent the proton on PropA of heme a_3 from going to the binuclear center rather than to the outside in the proton

expulsion steps. This can probably be arranged by having a rather high barrier for proton transfer between these positions. Again, a detailed study of possible proton transfers is necessary to reach further conclusions about this problem.

Acknowledgment. We are grateful for many interesting and useful discussions with Mårten Wikström, Håkan Wennerström, and Peter Brzezinski.

References and Notes

- (1) Ostermeier, C.; Harrenga, A.; Ermler, U.; Michel, H. *Proc. Natl. Acad. Sci. U.S.A.* **1997**, *94*, 10547–10553.
- (2) Yoshikawa, S.; Shinzawa-Itoh, K.; Nakashima, R.; Yaono, R.; Yamashita, E.; Inoue, N.; Yao, M.; Fei, M. J.; Libeu, C. P.; Mizushima, T.; Yamaguchi, H.; Tomizaki, T.; Tsukihara, T. *Science* **1998**, *280*, 1723–1729.
- (3) Svensson-Ek, M.; Abrahamson, J.; Larsson, G.; Tørrnroth, S.; Brzezinski, P.; Iwata, S. *J. Mol. Biol.* **2002**, *321*, 329–339.
- (4) Wikström, M. *Nature* **1977**, *266*, 271–273.
- (5) Wikström, M.; Jasaitis, A.; Backgren, C.; Puustinen, A.; Verkhovsky, M. I. *Biochim. Biophys. Acta* **2000**, *1459*, 514–520.
- (6) Gennis, R. B. *Proc. Natl. Acad. Sci. U.S.A.* **1998**, *95*, 12747–12749.
- (7) Ferguson-Miller, S.; Babcock, G. *Chem. Rev.* **1996**, *96*, 2889–2907.
- (8) Michel, H.; Behr, J.; Harrenga, A.; Kannt, A. *Annu. Rev. Biophys. Biomol. Struct.* **1998**, *27*, 329–356.
- (9) Morgan, J. E.; Verkhovsky, M. I.; Palmer, G.; Wikström, M. *Biochemistry* **2001**, *40*, 6882–6892.
- (10) Wikström, M. *Nature* **1989**, *338*, 776–778.
- (11) Michel, H. *Proc. Natl. Acad. Sci. U.S.A.* **1998**, *95*, 12819–12824.
- (12) Ruitenbergh, M.; Kannt, A.; Bamberg, E.; Fendler, K.; Michel, H. *Nature* **2002**, *417*, 99–102.
- (13) Verkhovsky, M. I.; Jasaitis, A.; Verkhovskaya, M. L.; Morgan, J. E.; Wikström, M. *Nature* **1999**, *400*, 480–483.
- (14) Iwata, S.; Ostermeier, C.; Ludwig, B.; Michel, H. *Nature* **1995**, *376*, 660–669.
- (15) Morgan, J. E.; Verkhovsky, M. I.; Wikström, M. *J. Bioenerg. Biomembr.* **1994**, *26*, 599–608.
- (16) Wikström, M.; Morgan, J. E.; Verkhovsky, M. I. *J. Bioenerg. Biomembr.* **1998**, *30*, 139–145.
- (17) Wikström, M. *Biochim. Biophys. Acta* **2000**, *1482*, 1–11.
- (18) Michel, H. *Biochemistry* **1999**, *38*, 15129–15140.
- (19) Becke, A. D. *Phys. Rev.* **1988**, *A38*, 3098. Becke, A. D. *J. Chem. Phys.* **1993**, *98*, 1372. Becke, A. D. *J. Chem. Phys.* **1993**, *98*, 5648.
- (20) Hay, P. J.; Wadt, W. R. *J. Chem. Phys.* **1985**, *82*, 299.
- (21) Blomberg, M. R. A.; Siegbahn, P. E. M.; Babcock, G. T. *J. Am. Chem. Soc.* **1998**, *120*, 8812–8824.
- (22) *Jaguar 4.0*; Schrödinger, Inc.: Portland, OR, 1991–2000.
- (23) Curtiss, L. A.; Raghavachari, K.; Redfern, R. C.; Pople, J. A. *J. Chem. Phys.* **2000**, *112*, 7374–7383.
- (24) Siegbahn, P. E. M.; Blomberg, M. R. A. *Annu. Rev. Phys. Chem.* **1999**, *50*, 221–249.
- (25) Siegbahn, P. E. M.; Blomberg, M. R. A. *Chem. Rev.* **2000**, *100*, 421–437.
- (26) Siegbahn, P. E. M.; Blomberg, M. R. A. *J. Phys. Chem. B* **2001**, *105*, 9375–9386.
- (27) Siegbahn, P. E. M. *Q. Rev. Biophys.* **2003**, *36*, 91–145.
- (28) Blomberg, M. R. A.; Siegbahn, P. E. M.; Babcock, G. T.; Wikström, M. *J. Inorg. Biochem.* **2000**, *80*, 261–269.
- (29) Blomberg, M. R. A.; Siegbahn, P. E. M.; Babcock, G. T.; Wikström, M. *J. Am. Chem. Soc.* **2000**, *122*, 12848–12858.
- (30) Zaslavsky, D.; Kaulen, A. D.; Smirnova, I. A.; Vygodina, T.; Konstantinov, A. A. *FEBS Lett.* **1993**, *336*, 389–393.
- (31) Proshlyakov, D. A.; Pressler, M. A.; Babcock, G. T. *Proc. Natl. Acad. Sci. U.S.A.* **1998**, *95*, 8020–8025.
- (32) Karpefors, M.; Ådelroth, P.; Namslauer, A.; Zhen, Y.; Brzezinski, P. *Biochemistry* **2000**, *39*, 14664.
- (33) Blomberg, M. R. A.; Siegbahn, P. E. M.; Wikström, M. *Inorg. Chem.* **2003**, *42*, 5231–5243.
- (34) Siegbahn, P. E. M.; Blomberg, M. R. A. *Biochim. Biophys. Acta*, in press.